

RESEARCH ARTICLE

The calculated rovibronic spectrum of scandium hydride, ScH

Lorenzo Lodi, Sergei N. Yurchenko and Jonathan Tennyson

*Department of Physics & Astronomy, University College London, London WC1E 6BT,
United Kingdom**(received December 19, 2021)*

The electronic structure of six low-lying electronic states of scandium hydride, $X^1\Sigma^+$, $a^3\Delta$, $b^3\Pi$, $A^1\Delta$, $c^3\Sigma^+$, and $B^1\Pi$, is studied using multi-reference configuration interaction as a function of bond length. Diagonal and off-diagonal dipole moment, spin-orbit coupling and electronic angular momentum curves are also computed. The results are benchmarked against experimental measurements and calculations on atomic scandium. The resulting curves are used to compute a line list of molecular ro-vibronic transitions for ^{45}ScH .

Keywords: diatomics; electronic structure; rovibronic transitions

Acknowledgment This work was supported by the ERC under Advanced Investigator Project 267219.

1. Introduction

Scandium hydride was first identified experimentally by Smith [1], who recorded the absorption spectra of various transition metal hydrides (ScH, TiH, VH, NiH, CoH and deuterated isotopologues) in the region 17700 to 18300 cm^{-1} . No detailed analysis of the spectrum was reported but it was remarked that a triplet ground state was expected. Later studies showed that the ground state of ScH is actually $^1\Sigma^+$, with a low-lying $^3\Delta$. Early studies using restricted open-shell Hartree-Fock (ROHF) [2, 3], generalised valence bond theory [4] and empirically-fitted pseudopotentials [5] all incorrectly predicted a $^3\Delta$ ground state, with the $^1\Sigma^+$ generally lying about 2000 cm^{-1} higher up. These studies considered the six electronic terms correlating upon dissociation with ground state atoms (dissociation channel labelled 1 in table 1, leading to $^1,3\Sigma$, $^1,3\Pi$ and $^1,3\Delta$); it was remarked [4] that the bonding of the molecular terms other than $^1\Sigma^+$ is due to the Sc(4s) and H(1s) orbitals, while the scandium 3d orbitals are relatively unaffected with respect to the atomic state [6]. On the other hand the bonding of $^1\Sigma^+$ was put down to *spd* bonding [4, 7]. The different bonding character of the $^1\Sigma^+$ term is probably one of the reasons why an extensive treatment of electron correlation is necessary to obtain the right ordering of the electronic terms. Bauschlicher and Walch [8] were

the first to correctly predict $^1\Sigma^+$ lying below $^3\Delta$ by performing full-valence multi-configuration self-consistent-field (MCSCF) calculations. Jeung and Koutecký [9] studied the same six electronic terms using pseudopotentials and truncated MRCI and confirmed a ground $^1\Sigma^+$ term close to equilibrium ($r_e \approx 3.4 a_0$), although for longer bond lengths $^3\Delta$ becomes lower in energy. Note that all these studies kept the scandium outer-core $3s3p$ electrons uncorrelated and often did not include relativistic corrections.

Anglada *et al* produced a series of papers [10–13] studying in great detail ScH and ScH⁺ using multi-reference configuration interaction (MRCI); in particular their final paper [13] constitutes the most complete theoretical study of ScH currently available. These authors confirmed that $^1\Sigma^+$ is the ground state when correlation effects are included; they also found that correlation of the Sc($3s3p$) semi-core electrons leads to large energy shifts, strongly stabilising the $^1\Sigma^+$ term with respect to the others and swapping the order of some of the excited states. They used basis sets similar in size to cc-pVTZ.

More recent theoretical studies considered ScH in the context of calibration studies of transition metal molecules using density function theory [14, 15], but they focused on equilibrium properties of very few terms and are of little relevance for us. An exception is the very recent study by Hubert *et al* [16] in which a detailed study of the ground $^1\Sigma^+$ and of two excited terms $^1,^3\Delta$ around equilibrium was presented and a modification of the coupled cluster method called general active space coupled cluster (GAS-CC) was used.

The only theoretical dipole moment data available for ScH are those by Anglada *et al* [13] and by Chong *et al* [17].

Experimentally a study by Bernard *et al* [18] reported three new bands ascribed to ScH and ScD in the region 11600 to 12700 cm⁻¹, but no detailed analysis or assignments were made due to the limited resolution and complexity of the spectra. More recently Ram and Bernath [19, 20] reported two detailed emission spectra analyses for ScH and ScD. In these studies they reported on singlet-singlet bands in regions from 5400 to 20500 cm⁻¹ assigned to transitions between 8 electronic terms, namely $X^1\Sigma^+$, $A^1\Delta$, $B^1\Pi$, $C^1\Sigma^+$, $D^1\Pi$, $E^1\Delta$, $F^1\Sigma^-$ and $G^1\Pi$. Two additional strong bands near 11620 and 12290 cm⁻¹ and two weaker bands near 12660 and 16845 cm⁻¹ were recorded but only incompletely analysed; the band near 11620 cm⁻¹ was conjectured to be due to a transition to the low-lying $^3\Delta$ term from a $^3\Phi$ term. Le and Steimle [21] reported more recently a detailed experimental study of the $X^1\Sigma^+ - D^1\Pi$ band around 16850 cm⁻¹, where also the electric dipole moments of ScH in its $X^1\Sigma^+$ and $D^1\Pi$ states were obtained using optical Stark spectroscopy. Very recently, Mukund *et al* [22] reported the observation of ScH emission bands at about 17900 cm⁻¹, ascribed to the $g^3\Phi - a^3\Delta$ triplet-triplet transitions.

This paper focuses on the six low-energy electronic states dissociating to ground state Sc and H atoms. Of the various experimentally observed bands [19–21] only $X - B$ is considered in the present study, although experiment is used for the empirical refinement of the potential energy curves of the singlet terms $X^1\Sigma$, $A^1\Delta$

and $B^1\Pi$ as well.

As part of the ExoMol project [23], whose aim is to produce comprehensive line lists for hot, astrophysically-important molecules, we have been constructing rovibrational and rovibronic line lists for a number of diatomic species [24–28]. However, so far none of these have contained a transition metal (TM). The richness of the spectrum of TM-containing diatomics makes their opacity particularly important for astrophysical studies [29] but treating their rovibronic spectrum *ab initio* is very challenging. Scandium hydride is the lightest TM molecule and for this reason constitutes a useful benchmark system for theoretical studies of such systems.

Scandium hydride has received comparatively little attention with respect to other transition metal hydrides such as FeH or NiH, in all probability because of the low abundance of scandium. Scandium is in fact the rarest of fourth-period transition metals (Sc–Zn) in the solar system [30], although it is more abundant than all heavier elements starting from the fifth period. The study presented here on ScH constitutes a first step in the *ab initio* calculation of ro-vibronic spectra of TM-containing molecule. We perform a series of *ab initio* calculations on both the scandium atom and ScH and use these to produce a line list of scandium hydride line positions and intensities which is reasonably complete in the region up to 12 000 cm^{-1} .

2. Atomic Scandium

As a preliminary test we studied in some detail the scandium atom using complete active space self consistent field (CASSCF) and internally-contracted MRCI calculations using the program Molpro [31].

We collected in table 1 reference energy levels of the scandium atom up to about 20 000 cm^{-1} , along with the ScH molecular terms correlating adiabatically with the various atomic states; this information serves as an indication of which molecular terms are expected to be low-lying; the rationale is that for transition-metal hydrides the hydrogen atom constitutes a relatively small perturbation of the atomic energy levels, so that molecular terms correlating with high-energy atomic products should be high-lying too. The lowest dissociation channel is separated by about 11 500 cm^{-1} from others, and in fact the six electronic terms correlating to it are lowest-lying and most theoretical studies concentrated on them. The dissociation channels 1 to 10 reported in table 1 lead altogether to 60 electronic molecular terms; that is, there are 60 energy curves in absence of spin-orbit splitting, which become 155 in presence of spin-orbit splitting. Of these, only eight have been characterised experimentally [20]. Very probably many of the remaining molecular energy curves are repulsive (i.e., have no minimum) and therefore do not concern us here. In any case great complexity and strong perturbations in the observed spectra are expected. This is typical of open-shell transition metal molecules.

In the following we consider the excitation energies from the ground 2D term

Table 1. Energy levels for scandium atom up to 20 200 cm^{-1} . The $\langle E \rangle$ are term-averaged energies, computed by $\langle E \rangle = \frac{\sum_J (2J+1) E_J}{\sum_J (2J+1)}$; experimental energies for the levels E_J where taken from the NIST website [32]. $n_f = \min(2S+1, 2L+1)$ is the number of fine-structure components of a given terms due to spin-orbit interaction; $n_\mu = (2S+1)(2L+1)$ is the total degeneracy of the term (number of microstates). The ξ 's are effective spin-orbit coupling constants, such that the spin-orbit splittings for each term are best reproduced by the expression $E_J = E_0 + \xi[(J(J+1) - L(L+1) - S(S+1))/2, J = |L-S|, \dots, L+S]$. The last column lists the molecular terms for ScH correlating at dissociation with the given Sc atomic term plus a ground state ^2S hydrogen atom.

#	config.	term	$\langle E \rangle / \text{cm}^{-1}$	n_f	n_μ	ξ / cm^{-1}	molecular terms
1	$3d^1 4s^2$	^2D	0.0	2	10	67.3	$1,3[\Sigma^+, \Pi, \Delta]$
2	$3d^2 4s^1$	^4F	11 509.1	4	28	15.0	$3,5[\Sigma^-, \Pi, \Delta, \Phi]$
3	$3d^2 4s^1$	^2F	14 891.3	2	14	33.1	$1,3[\Sigma^-, \Pi, \Delta, \Phi]$
4	$3d^1 4s^1 4p^1$	$^4\text{F}^\circ$	15 775.8	4	28	33.6	$3,5[\Sigma^+, \Pi, \Delta, \Phi]$
5	$3d^1 4s^1 4p^1$	$^4\text{D}^\circ$	16 031.0	4	20	25.2	$3,5[\Sigma^-, \Pi, \Delta]$
6	$3d^1 4s^1 4p^1$	$^2\text{D}^\circ$	15 951.4	2	10	-29.7	$1,3[\Sigma^-, \Pi, \Delta]$
7	$3d^2 4s^1$	^2D	16 916.7	2	10	-5.0	$1,3[\Sigma^+, \Pi, \Delta]$
8	$3d^2 4s^1$	^4P	17 175.2	3	12	20.1	$3,5[\Sigma^-, \Pi]$
9	$3d^1 4s^1 4p^1$	$^4\text{P}^\circ$	18 440.6	3	12	15.0	$3,5[\Sigma^+, \Pi]$
10	$4s^2 4p^1$	$^2\text{P}^\circ$	18 706.5	2	6	96.5	$1,3[\Sigma^+, \Pi]$

to the two lowest-energy excited terms, namely ^4F and ^2F . We expect that errors of computed molecular excitation energies are comparable with the corresponding error in the atomic case.

The most accurate study of (neutral or singly-ionized) transition metal atoms including scandium is due to Balabanov and Peterson [33, 34]. These authors used coupled cluster up to CCSDTQ, relativistic corrections based on the Douglas-Kroll-Hess (DKH) hamiltonian, included core correlation and developed the largest basis sets available for transition metals. For scandium $^2\text{D} \rightarrow ^4\text{F}$ excitation energy the best theoretical coupled cluster result is higher than the experimental one by about 115 cm^{-1} . The corresponding result using ACPF (a multi reference method very close to MRCI) in conjunction with the full-valence reference space is too low by about 110 cm^{-1} ; using a larger reference space including a further set of diffuse d functions (which are thought to be necessary for describing the late transition metals Fe-Cu) leads to a worse agreement with experiment of about 190 cm^{-1} . Other recent studies of transition metal atoms excitation energies including scandium were performed by Raab and Roos [35] and Mayhall *et al* [36]. Raab and Roos [35] computed the $^2\text{D} \rightarrow ^4\text{F}$ excitation energy with CCSD(T) and CASPT2 using the DKH hamiltonian for relativistic effects and the ANO-RCC basis set (similar in size to aug-cc-pCVQZ). Both CCSD(T) and CASPT2 frozen core values agree with experiment to about 250 cm^{-1} , but allowing for core correlation worsens somewhat the agreement to about 500 cm^{-1} . Mayhall *et al* [36] also used core-correlated CCSD(T) with the G3Large basis set (similar in size to aug-cc-pCVTZ) and reported an agreement of 250 cm^{-1} without inclusion of relativistic effects and of about 1200 cm^{-1} when relativistic effects were included.

Table 1 gives some indicative result for both the $^2\text{D} \rightarrow ^4\text{F}$ and $^2\text{D} \rightarrow ^2\text{F}$ transitions performed in this study using MRCI and the full valence reference space. Our

Table 2. Electronic term excitation energies for scandium atom (this work). All calculations used the full-valence (3-electron, 9-orbital) complete active space comprising the $3d4s4p$ orbitals. Orbitals are state-averaged over the three electronic terms considered. MRCI+Q are Davidson-corrected energies (relaxed reference). Calculated values are reported as (reference – calculated), and reference energies are taken from the column labelled ‘ $\langle E \rangle$ ’ of table 1. All quantities are in cm^{-1} .

Method		$^2D \rightarrow ^4F$	$^2D \rightarrow ^2F$
reference energies=		11 509.1	14 891.3
		ref - calc	
CASSCF	3z	28.6	64.0
CASSCF	4z	49.2	86.0
MRCI/frz core	3z	-1187.9	-421.8
MRCI/frz core	4z	-1084.6	-265.3
MRCI/core corr	wc3z	573.3	541.1
MRCI/core corr	wc4z	1072.1	1056.0
MRCI+Q/core corr	wc4z	2080.0	2039.8
MRCI+Q/core corr/DKH4	wc4z-DK	813.6	707.1

best results for both transitions are too small on the average by about 750 cm^{-1} with respect to the results by Balabanov and Peterson; our errors are larger probably because we performed a state-averaged calculation at the CASSCF level and also because of the smaller basis sets used. A striking consideration is that the non-relativistic CASSCF excitation energies are extremely good, a fact which can only be due to fortuitous cancellation of errors. Overall our results and the analysis of the literature show that it is difficult to get excitation energies correct to better than about 500 cm^{-1} , and that good agreement with experiment can be often due to cancellation effects. We also observed that the relativistic contribution to excitation energies shows relatively large variations of the order of 500 cm^{-1} depending on the levels of electron correlation (CASSCF, MRCI valence only or core-correlated) and on using the mass-velocity one-electron Darwin (MVD1) rather than the Douglas-Kroll-Hess (DKH) Hamiltonian.

We also computed atomic spin-orbit splitting constants using CASSCF and MRCI wave functions as implemented in MOLPRO. Results are collected in table 3. Spin orbit splitting constants show weak sensitivity to the size of the basis set and already with the smallest 2z basis set are converged within 1 cm^{-1} . The dependence on the electron correlation treatment is also weak, with the ground 2D term being the most sensitive. Going from CASSCF to frozen-core MRCI increases $\xi(^2D)$ by $+18 \text{ cm}^{-1}$ but reduces $\xi(^4F)$ and $\xi(^2F)$ by only 1.5 and 0.9 cm^{-1} respectively. Correlating the $(3s3p)$ outer core increases $\xi(^2D)$ by 5 cm^{-1} , $\xi(^4F)$ by 1.8 cm^{-1} and $\xi(^2F)$ by 2.6 cm^{-1} . With respect to the experimentally-derived values we do not observe a clear pattern of convergence with respect to the level of theory used, and the simplest CASSCF/2z values agree with experiment practically as well as the core-correlated, large basis set MRCI ones.

Table 3. Calculated spin-orbit constants ξ for scandium atom. The column labelled ‘obs.’ are experimentally derived values from table 1. All values are in cm^{-1} .

CASSCF					
transition	Obs.	2z	3z	4z	5z
$\xi(^2D)$	67.3	57.5	57.6	57.9	57.9
$\xi(^4F)$	15.0	18.5	18.5	18.6	18.6
$\xi(^2F)$	33.1	37.2	37.2	37.4	37.4

MRCI (frz. core)					
transition		2z	3z	4z	5z
$\xi(^2D)$	67.3	74.7	75.6	76.0	76.0
$\xi(^4F)$	15.0	16.8	17.0	17.1	17.1
$\xi(^2F)$	33.1	35.9	36.4	36.5	36.6

MRCI (core correlated)					
transition		wc3z	wc4z	wc5z	
$\xi(^2D)$	67.3	80.3	81.2	81.3	
$\xi(^4F)$	15.0	18.7	18.9	19.0	
$\xi(^2F)$	33.1	38.6	39.1	39.2	

Considering that errors of $\approx 5 \text{ cm}^{-1}$ in spin-orbit couplings are very small with respect to the error in the main non-relativistic energies we conclude that it is quite acceptable to compute spin-orbit couplings at a low level of theory.

3. ScH molecule

As discussed in the introduction and hinted by the results for the Sc atom presented in the previous section, from the point of view of high-resolution spectroscopy the accuracy expected for transition metal diatomics is much lower than the one generally achievable for molecules made up by main-group atoms. Also, because convergence seems to be rather irregular both with respect to the level of electron correlation and basis set size, one should not necessarily expect more expensive calculations to be much closer to experiment than simpler ones.

For this reason, when possible, experimental data were used to adjust the *ab initio* potential energy curves, in particular, the experimental studies by Ram and Bernath [19, 20] where the $v = 0$ and sometimes $v = 1$ and $v = 2$ vibrational states of seven singlet terms ($X^1\Sigma^+$, $A^1\Delta$, $B^1\Pi$, $C^1\Sigma^+$, $D^1\Pi$, $F^1\Sigma^-$ and $G^1\Pi$) were characterised. Of these the X , A and B terms dissociate to channel 1 of table 1, C to channel 7 or perhaps 10, F to channel 6 while for terms D and G channels 3, 6, 7, or 10 are all possible on the basis of symmetry considerations.

Details on the refinement are given in section 4; in the rest of this section we discuss the *ab initio* calculations.

3.1. Potential energy curves

Energy curves for the six molecular electronic terms correlating with the ground atomic states (dissociation channel 1 of table 1) were computed using CASSCF and internally-contracted MRCI [37] in conjunction with the recent aug-cc-pwCVnZ basis sets (awcnz for short) [33, 34]. CASSCF orbitals (state-averaged over all the degenerate components of the six terms considered in this work) were used as a basis of the MRCI runs.

A four-electron, ten-orbital complete active space comprising the scandium $4s, 3d, 4p$ orbitals and the hydrogen $1s$ orbital (5 active orbitals of a_1 symmetry, 2 b_1 , 2 b_2 and 1 a_2 in the C_{2v} point group) was used in the calculations. The outer-core scandium $3s, 3p$ orbitals were left doubly occupied at the CASSCF stage but were correlated at the MRCI one. The inner-core $1s, 2s, 2p$ orbitals were not correlated. As discussed by Balabanov and Peterson [34], in multireference calculations the late transition metals Fe-Cu require an active space larger than the full-valence one, which should include a further set of diffuse d functions. However this is not necessary for scandium. Inclusion of the Sc $4p$ orbitals is not thought to be indispensable for a correct description of bonding but was found to be necessary in practice to avoid convergence problems at the CASSCF stage. All curves were computed in the range 2.0 to 8.5 a_0 in steps of 0.05 a_0 and from 9.0 to 13.5 a_0 in steps of 0.5 a_0 , for a total of 141 points.

Our best *ab initio* results are based on MRCI using the awc5z basis set; computing at this level the energies for all six terms for a single geometry takes about 4 GB of RAM, 20 GB of disk space and 12 hours on a single core of an Intel Xeon E5-2670 CPU at 2.60 GHz. Potential energy curves include a relativistic correction computed as expectation value of the MVD1 operator. The Davidson correction was not included in our final *ab initio* curves because, as already registered for the excitation energies of the scandium atom (see table 2), it does not improve agreement with known experimental data; furthermore tests (not discussed here in detail) at the frozen-core / cc-pVDZ level showed that Davidson-corrected energies agreed worse with full CI than uncorrected MRCI ones.

The *ab initio* energy curves were slightly shifted in energy (i.e., their T_e were changed) so that they are exactly degenerate upon dissociation; in our MRCI calculation the exact degeneracy of the terms at $r = +\infty$ is broken mainly because the energies of (singlet or triplet) Σ^+ and Δ terms is computed simultaneously with a two-state calculation, while the (singlet or triplet) Π terms were computed with one-state calculations; because of the internal contraction approximation used in Molpro in a multi-state calculation the variational flexibility of the MRCI wave function is increased and this results in a small downwards shift in energy. As a consequence at dissociation the two Π terms are about 50 cm^{-1} higher in energy than the other terms; furthermore a small breaking of exact degeneracies is expected and normal also in uncontracted MRCI calculations because of the incomplete treatment of electron correlation. We therefore thought it was reasonable to shift all terms to restore the exact degeneracy. The shifts applied to MRCI/awc5z/MVD1

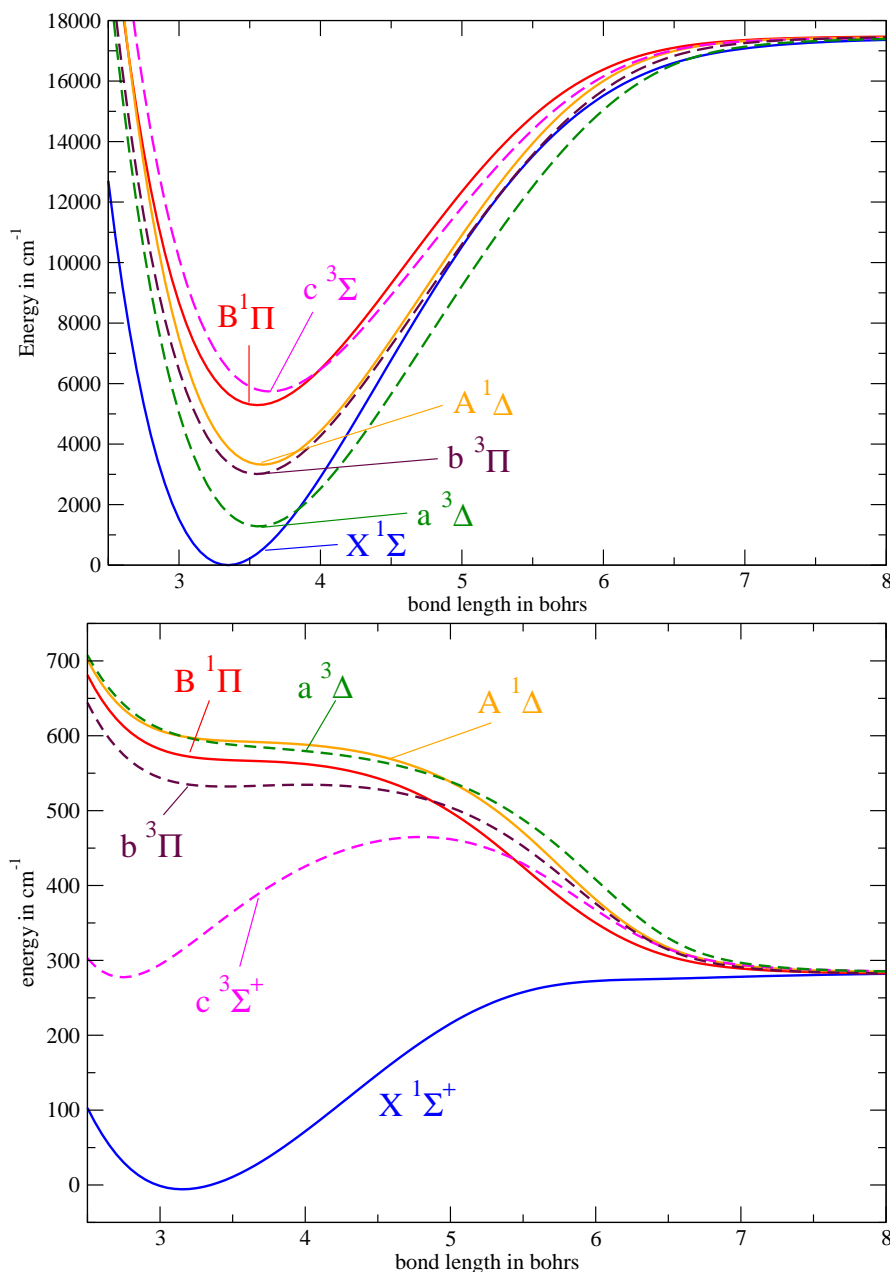


Figure 1. *Ab initio* potential curves for ScH computed with MRCI and the awc5z basis set and the corresponding relativistic MVD1 correction curves (see text for details). The $3s3p$ orbitals were correlated.

curves for the $A^1\Delta$, $B^1\Pi$, $a^3\Delta$, $b^3\Pi$ and $c^3\Sigma^+$ terms are respectively 1.1, 49.7, 1.5, 49.9 and 2.1 cm^{-1} . The ground $X^1\Sigma^+$ term was taken as a reference and not shifted.

Figure 1 presents our computed potentials. As it can be seen the ground $X^1\Sigma^+$ curves are distinct from the other curves: it has a much shorter equilibrium bond length and its relativistic correction curve is also very different from the others. This is a consequence of the different bonding character of this $X^1\Sigma^+$ term discussed in section 1.

Equilibrium bond lengths r_e , harmonic vibrational frequencies ω_e and adiabatic

Table 4. Computed *ab initio* adiabatic electronic excitation energies (in cm^{-1}), equilibrium bondlengths (in a_0) and harmonic frequencies (in cm^{-1}) for selected ScH electronic terms.

Term	Anglada et al ^a			Hubert et al ^b			This work ^c		
	T_e	r_e	ω_e	T_e	r_e	ω_e	T_e	r_e	ω_e
$X^1\Sigma^+$	0	3.41	1621	0	3.35	1611	0	3.34	1587
$A^1\Delta$	6600	3.68	1541	5362	3.58	1439	3914	3.59	1428
$B^1\Pi$	8400	3.64	1451	—	—	—	5856	3.55	1380
$a^3\Delta$	4600	3.66	1460	3660	3.55	1450	1868	3.56	1432
$b^3\Pi$	6200	3.64	1438	—	—	—	3544	3.55	1406
$c^3\Sigma^+$	7900	3.68	1389	—	—	—	6122	3.63	1325

^a Ref. [13]; values of the T_e 's are taken from the column labelled 'B(1f)' of table 8, r_e 's and ω_e 's from table 10.

^b Ref. [16], using the data from the column labelled CCSDT12 (Q ζ) of Table V and adding the relativistic corrections in the last column of Table VI.

^c Using MRCI/awc5z/MVD1. The $\omega_e^{(i)}$ relative to state i was computed by $\omega_e^{(i)} = \sqrt{V''(r_e^{(i)})/\mu}$ while the adiabatic excitation energy $T_e^{(i)}$ was computed as $V_i(r_e^{(i)}) - V_0(r_e^{(0)})$, where V_0 is the potential for the $^1\Sigma^+$ ground state.

excitation energies T_e are reported in table 4 and compared with previous theoretical calculations.

Our computed equilibrium bond lengths are in very good agreement (within 0.01 a_0) with the recent theoretical values by Hubert *et al* [16].

We compare our *ab initio* and empirically-refined results with energy levels reconstructed from the experimental study [20] in table 5; empirical refinement is discussed in section 4. We prefer to compare directly with experimental energy levels because experimentally-deduced values for T_e , r_e and ω_e also include in an effective way spin-orbit and other coupling effects between different electronic terms.

As discussed above, we expect our computed adiabatic excitation energies T_e to have errors of several hundreds or perhaps a few thousands of cm^{-1} and therefore they cannot be considered very accurate. On the other hand the equilibrium bond lengths and the shape of the potentials should be reasonably accurate, see also table 5, where the accuracy of the potential energy curves of the singlet states can be assessed by comparing to the vibrational energy separations within each state. The rotational intervals between the two lowest- J $v = 0$ energy levels are reproduced by our *ab initio* curves with errors of 0.00, 0.12 and 0.28 cm^{-1} for the X , A and B term respectively. Errors in vibrational transitions $v = 0$ to $v = 0$ are 8.44 cm^{-1} for the X term and 29.27 cm^{-1} for the B term.

For the ground X term only, we considered the error of the coupled-cluster based potential curves. The absolute errors for the $v = 0$ to $v = 1$ transition wavenumber using CCSD, CCSD(T), CCSDT and CCSDT(Q) are, respectively, 54.73, 24.45, 6.75 and 1.15 cm^{-1} with the awc5z basis set, the DKH Hamiltonian and keeping all the coupling terms computed with MRCI or CASSCF; the CCSDT and CCSDT(Q) curves were obtained in the basis set formed by wc3z for Sc and 2z for hydrogen, and

Table 5. Selected energy levels for the lowest-energy singlet terms of ScH in cm^{-1} . J is the total angular momentum (neglecting nuclear spin), v is the vibrational quantum number, p the parity; ‘Obs.’ are the values derived using the spectroscopic constants reported by Ram and Bernath [20] and the program PGOPHER [38]; ‘A’ and ‘R’ are the term values calculated with Duo using the *ab initio* (MRCI/awc5z/MVD1) and *refined* curves as described in the text. Calculations included spin-orbit and other couplings between electronic terms.

J	p	energies			obs – calc	
		obs	<i>ab initio</i>	<i>refined</i>	<i>ab initio</i>	<i>refined</i>
$X^1\Sigma^+, v = 0$						
0	+	0.00	0.00	0.00	0.00	0.00
1	-	10.73	10.73	10.73	0.00	0.00
10	+	586.89	586.88	586.93	-0.04	-0.05
$X^1\Sigma^+, v = 1$						
0	+	1546.97	1538.53	1547.10	8.44	-0.12
1	-	1557.45	1549.00	1557.54	8.45	-0.09
10	+	2120.06	2111.48	2118.31	8.58	1.76
$A^1\Delta, v = 0$						
2	+	4213.36	3830.27	4213.35	383.09	0.01
3	+	4241.34	3858.12	4241.36	383.21	-0.03
10	+	4696.30	4311.04	4696.64	385.25	-0.34
10	-	4696.30	4311.01	4696.61	385.28	-0.31
$B^1\Pi, v = 0$						
1	+	5413.98	5704.18	5413.94	-290.19	0.04
2	+	5433.77	5723.68	5433.79	-289.91	-0.02
10	+	5943.02	6226.10	5939.67	-283.07	3.35
10	-	5939.42	6222.43	5936.36	-283.01	3.06
$B^1\Pi, v = 1$						
1	+	6776.75	7037.67	6776.70	-260.92	0.05
2	+	6795.96	7056.69	6796.35	-260.73	-0.39
10	+	7290.12	7546.50	7290.43	-256.38	-0.31
10	-	7286.57	7542.84	7286.95	-256.28	-0.38
$B^1\Pi, v = 2$						
1	+	8092.50	8323.48	8092.51	-230.98	-0.01
2	+	8111.15	8342.00	8111.07	-230.85	0.08
10	+	8590.66	8818.77	8589.10	-228.10	1.56
10	-	8587.14	8815.10	8585.06	-227.96	2.08

added as a correction to the CCSD(T) curve. These result indicate that our MRCI curves are, close to equilibrium, similar in quality to CCSDT and that quadruple excitations must be accounted for to obtain accuracies of the order of 1 cm^{-1} .

3.2. Dissociation energy

The dissociation energy D_0 of ScH is related to the potential well depth D_e by

$$D_0 = D_e - E_{\text{ZPE}} \quad (1)$$

where $E_{\text{ZPE}} = 787 \text{ cm}^{-1}$ is the zero-point rotational-vibrational energy and the quoted value was computed using out MRCI/awc5z/MVD1 PEC. The potential well depth D_e can be decomposed into three contributions: a main non-relativistic one, a spin-independent (scalar) relativistic contribution and a spin-dependent contribution due to spin-orbit:

$$D_e = D_e^{\text{NR}} + D_e^{\text{R}} + D_e^{\text{SO}} \quad (2)$$

The spin-orbit contribution D_e^{SO} is due to the energy lowering of the scandium atom $^2\text{D}_{3/2}$ level with respect to the ^2D term and has a value $D_e^{\text{SO}} = -3\xi/2 = -101 \text{ cm}^{-1}$, where $\xi = 67.3 \text{ cm}^{-1}$ is the atomic spin-orbit constant for the ^2D term (see table 1).

The (spin-orbit free) potential well depth D_e^{NR} computed with MRCI/awc5z is 17459 cm^{-1} ; the Davidson correction gives a rather large shift of $+1355 \text{ cm}^{-1}$, leading for MRCI+Q/awc5z to a value $D_e^{\text{NR}} = 18814 \text{ cm}^{-1}$.

With a view to ascertaining the quality of our *ab initio* curve close to dissociation we computed an accurate value for D_e^{NR} using high-order coupled cluster and the program MRCC [39].

Using the awc5z basis set and correlating the outer-core $3s3p$ orbitals gives for $D_e^{\text{NR}} = 17694 \text{ cm}^{-1}$ using CCSD and 18547 cm^{-1} using CCSD(T). The effect of full triples (T) \rightarrow T was evaluated in a basis set formed by the wc3z for scandium and 2z for hydrogen, giving a shift of $+163 \text{ cm}^{-1}$. The effect of quadruple excitations was evaluated in an even smaller basis set constructed complementing the 2z one for hydrogen and scandium with the core-correlation functions taken from the wc3z basis set and dropping the g functions; the computed shift T \rightarrow Q is $+48 \text{ cm}^{-1}$; our best awc5z (frozen inner-core) coupled cluster value is $D_e^{\text{NR}} = 18547 + 163 + 48 = 18758 \text{ cm}^{-1}$. The coupled cluster value therefore strongly supports the Davidson-corrected value for D_e^{NR} rather than the uncorrected MRCI one.

We also considered the contribution to D_e^{NR} due to correlation of the inner-core $2s2p$ orbitals; this effect gives a contribution of $+62 \text{ cm}^{-1}$ using CCSD/awc5z and $+104 \text{ cm}^{-1}$ using CCSD(T)/awc5z.

The magnitude of basis set incompleteness was estimated by looking at the difference between the awc5z values and the basis set extrapolated ones using the awc4z and awc5z basis sets; Basis set extrapolation of the awc5z values gives a very small contribution, namely -3 cm^{-1} for MRCI/awc5z and $+6 \text{ cm}^{-1}$ for CCSD(T)/awc5z.

Finally, our best coupled-cluster-based value for the non-relativistic part of the potential well depth is $D_e^{\text{NR}} = 18758 + 104 + 6 = 18868(50) \text{ cm}^{-1}$, where the given uncertainty was assigned by halving of the sum of the quadruples correction, the difference between the CCSD and CCSD(T) inner-core corrections and the basis set extrapolation contribution.

We now consider the scalar relativistic contribution D_e^{R} . The MVD1/awc5z value is $D_e^{\text{R}} = +285 \text{ cm}^{-1}$; using the DKH Hamiltonian (truncated to fourth order) and the awc4z-DK basis gives a contribution $+311 \text{ cm}^{-1}$ using MRCI, $+291 \text{ cm}^{-1}$ using MRCI+Q and $+307 \text{ cm}^{-1}$ using CCSD(T).

Taking the DKH value $D_e^{\text{R}} = 307 \text{ cm}^{-1}$ (although there is no conclusive argument to favour it instead of the MVD1 one) we arrive at a final value for the potential well depth $D_e = 18868 + 307 - 101 = 19074(60) \text{ cm}^{-1}$ and to a dissociation energy $D_0 = 19074 - 787 = 18287(60) \text{ cm}^{-1}$, where the given uncertainty was increased to reflect the uncertainty on the relativistic correction.

Kant and Moon [40] reported long ago an experimental value for the potential well depth $D_e = 16613 \pm 700 \text{ cm}^{-1}$ and Koseki *et al* [41] gave a survey of calculated values of D_e which have a large spread of about 3000 cm^{-1} around the value quoted.

Our computed value is larger than the experimental one by about 2500 cm^{-1} and in disagreement with it by more than three times its uncertainty bar.

Finally, we report some run-times for our coupled cluster results. The CCSDT run using the $\text{wc}2\text{z}/2\text{z}$ basis set took for ScH 8.3 hours of CPU time on a 12-core Xeon X5660 at 2.80GHz machine (1.3 hours real time). The CCSDTQ run for ScH in the $2\text{z}+\text{wC}3\text{z}$ basis set took 10.6 days of CPU time (1.6 days real time) and 5 GB of RAM on the same machine. A single CCSD(T)/ $\text{awc}5\text{z}$ run takes about 10 minutes on a single core of the same machine.

3.3. Dipole moment curves

While potential energy curves can be refined semiempirically from (even limited) experimental data, one has normally to rely on computed, *ab initio* dipole moment curves [42]. With a view to computing accurate line intensities it is therefore important to produce dipole moment curves as accurate as possible.

Le and Steimle [21] reported for the ground $X^1\Sigma^+$ term an experimental equilibrium dipole $\mu = 1.74(0.15)$ D using optical Stark spectroscopy; for our work we choose the z axis such that a negative dipole corresponds to Sc^+H^- polarity, so we reverse their value to $\mu = -1.74(0.15)$ D.

We were able to produce a very accurate value for the equilibrium dipole of the ground state term using coupled cluster and the energy-derivative (ED) method [43] ($\lambda = \pm 10^{-4}$ au). As we are dealing with a closed-shell electronic state near equilibrium coupled cluster converges quickly with respect to the level of excitations included. High-order coupled cluster calculations used the program MRCC [39]. Results are collected in table 6; our best theoretical value is $\mu_e = -1.72(2)$ D and is in full agreement with the experimental value of Le and Steimle [21].

MRCI, on the other hand, has difficulties in reproducing the correct value for the dipole. Apart from the basis set size and whether or not core orbitals are correlated, we considered three further factors affecting MRCI dipoles, namely: *i*) whether dipoles are computed by expectation value (XP) or energy derivative (ED) [43]; *ii*) whether at the CASSCF step orbitals are obtained by state averaging (state-averaged orbitals, SAO) or are specifically optimised for the $X^1\Sigma^+$ electronic term (state-specific orbitals, SSO); and, *iii*), the effect of using Davidson-corrected energies instead of MRCI ones. We compared dipoles obtained with MRCI in the $\text{awc}3\text{z}$ basis set with the very accurate (non-relativistic, $3s3p$ correlated) value obtained with coupled cluster, which gives in this basis set the value $\mu = 1.66$ D (see table 6, CCSD(T)/ $\text{awc}3\text{z}$ value + lines B,C,D). Results are collected in table 7. Figure 2 shows the dipole moment curves for the X ground term computed with CCSD(T), MRCI/XP, MRCI/ED and MRCI+Q/ED; note that the CCSD(T) curve become unphysical at large bondlengths.

As one can see in table 7 both CASSCF and MRCI/XP equilibrium dipoles are too small in magnitude by about 0.3–0.5 D, a considerable amount; using state-specific orbitals reduces the error to about 0.3 D, indicating that the CASSCF and MRCI wave functions are quite far from the exact, full CI one (which is independent

Table 6. Equilibrium dipole of the ground state $X^1\Sigma^+$ term using coupled cluster theory. Dipoles were computed at $r = 3.35 a_0$ using the energy-derivative method and $\lambda = \pm 10^{-4}$ au. A part from the line labelled ‘D’, all calculations correlated the outer-core $3s3p$ orbitals but the kept the inner core $1s2s2p$ uncorrelated. Dipoles are in debyes. The experimental value is -1.74(0.15) D [21].

label	method	basis set	value
A	RHF	awc3z	-1.436
	CCSD	awc3z	-1.668
	CCSD(T)	awc3z	-1.640
	CCSD(T)	awc4z	-1.686
	CCSD(T)	awc5z	-1.702
	CCSD(T)	awc[345]z ^a	-1.719
higher order correlation			
B	(T) \rightarrow T	wc3z/2z ^b	-0.002
C	T \rightarrow T(Q)	wc3z/2z ^b	-0.009
D	T(Q) \rightarrow Q	2z+wc(3z) ^c	-0.005
inner-core correlation ^d			
E	CCSD(T)	awc3z	-0.011
relativistic ^e			
F	CCSD(T)	awc4z	+0.078
vibrational averaging ^f			
G			-0.054
A + B +C +D +E+F+G best <i>ab initio</i> ^g			-1.72(2)

^a Basis-set extrapolated value using a $\mu_n = \mu_e + A/n^3$ formula.

^b Correction due to full triples and perturbative quadruple excitations using the cc-pVDZ basis set for hydrogen and cc-pwCVTZ for scandium.

^c Correction due to full quadruple excitations using the cc-pVDZ basis set for hydrogen and the cc-pVDZ complemented with the core-valence correlation functions from the cc-pwCVTZ (g functions excluded) for scandium.

^d Correction due to correlation of the $2s2p$ orbitals. The innermost $1s$ orbital was not correlated.

^e Correction due to scalar-relativistic effects computed as difference of CCSD(T)/DKH4/awc5z-dk and CCSD(T)/awc5z dipoles.

^f Vibrational averaging computed as $\langle 0|\mu(r)|0\rangle - \mu(r = 3.35a_0)$, where $|0\rangle$ is the $J = 0, v = 0$ vibrational ground state (obtained using the *ab initio* MRCI/awc5z PEC) and $\mu(r)$ is the MRCI/energy-derivative/awc5z dipole moment curve.

^g The estimated uncertainty in the teoretical dipole is mostly due to residual basis set incompleteness error and incomplete treatment of higher-order correlation effects.

Table 7. Values and errors in computed MRCI dipoles at $r = 3.35$ a_0 for the ground state $X^1\Sigma^+$ term. The acronym SAO and SSO stand for state-averaged orbitals and state-specific orbitals, respectively. The last two columns report differences with the accurate value $\mu = 1.66$ D obtained with coupled cluster (see text). Dipoles are in debyes.

method ^a	values		values – exact	
	SAO	SSO	SAO	SSO
CASSCF/XP	-0.99	-1.32	0.67	0.34
MRCI/XP	-1.19	-1.35	0.47	0.31
MRCI/ED	-1.56	-1.66	0.08	0.00
MRCI+Q/ED	-1.68	-1.71	-0.02	-0.05

^a XP or ED specifies whether dipole were computed as expectation value or energy derivatives (field strength $\lambda = \pm 10^{-4}$ au).

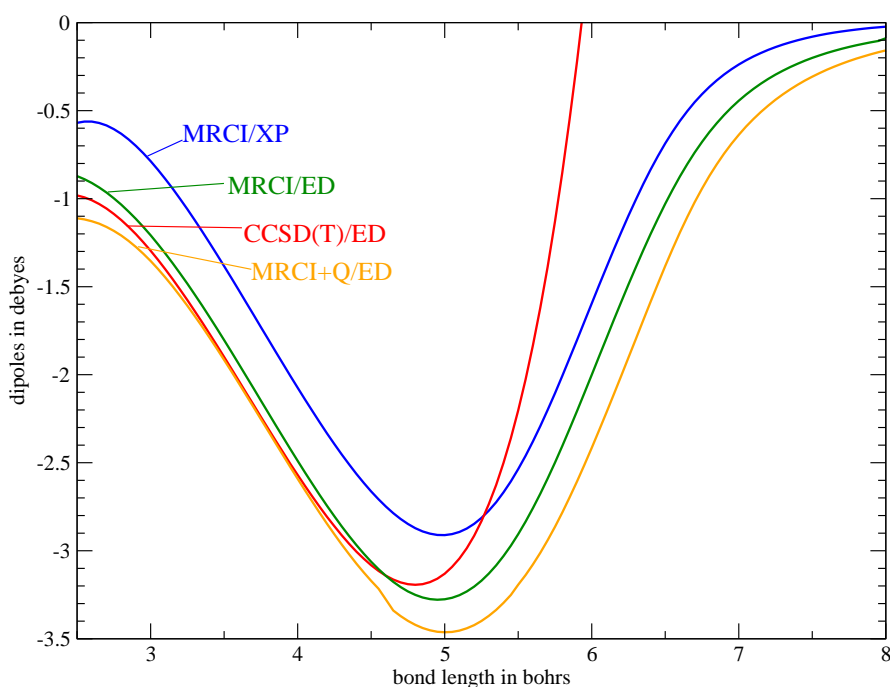


Figure 2. *Ab initio* dipole curves for the ground $X^1\Sigma^+$ term computed in the awc5z basis set and various methods (see text).

on the choice of the orbitals). Computing the dipole by energy derivative greatly reduces the error in the MRCI dipoles, bringing them in much closer agreement with the coupled cluster value. Using Davidson-corrected energies (MRCI+Q) introduces a shift of about 0.12 D and brings the dipole curve near equilibrium even closer to the coupled cluster one (see also fig. 2). The Davidson-corrected dipole curve (‘relaxed’ reference energies were used) has a small jump discontinuity (0.02 D of magnitude) at $r = 4.6$ a_0 ; on the other hand the MRCI/ED curve is perfectly smooth for all bond lengths. In conclusion the major factor affecting MRCI dipoles is whether the XP or ED technique is used, with ED producing considerably better dipoles. Using SSO instead of SSA helps somewhat but is of secondary importance.

It is also worth noting that, although the absolute value of MRCI/XP dipoles

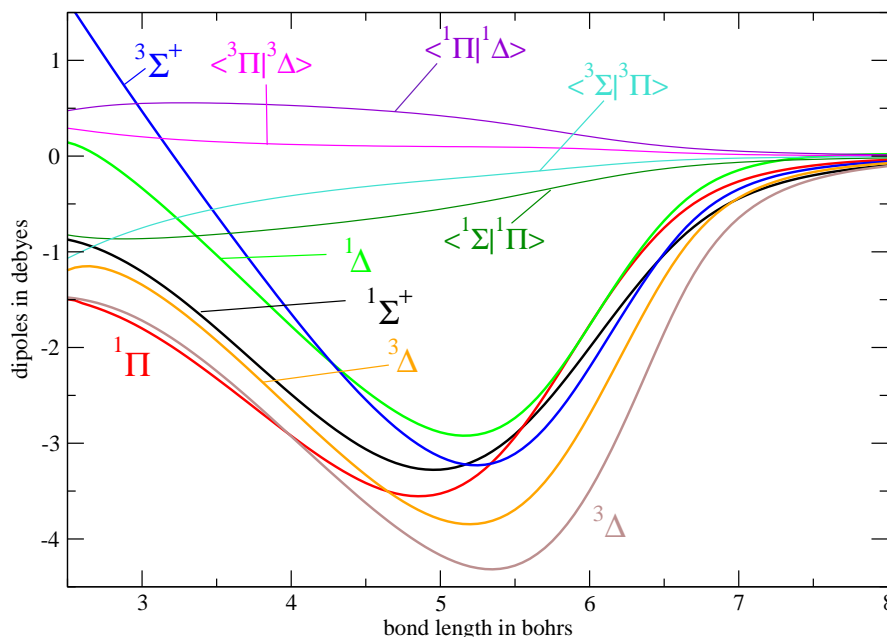


Figure 3. Diagonal (in bold) and off-diagonal dipole moment curves for ScH computed with with MRCI and the awc5z basis set.

is considerably off, this quantity only affects line intensities for pure rotational transitions. Intensities of vibrational transition within an electronic term depend on the shape of the dipole function, and may be given quite accurately even by MRCI/XP.

Finally, we decided to use awc5z/MRCI/ED for all diagonal dipole curves in virtue of their smoothness, although using MRCI+Q dipoles may lead to a slight improvement. Off-diagonal dipoles were computed as expectation values of the awc5z/MRCI wave functions; although it is possible to compute off-diagonal dipoles using an energy-derivative technique [44], this route was not pursued at this time. Figure 3 shows the diagonal and off-diagonal dipole moment curves for the various electronic.

3.4. Spin-orbit and other coupling curves

We computed spin-orbit couplings and couplings of the angular momentum operators \hat{L}_x and \hat{L}_y using the CASSCF or MRCI wave functions.

Figure 4 shows matrix elements of the L_x and L_y operator, obtained at the CASSCF/awc3z level; these couplings enter in the L -uncoupling and spin-electronic terms of the rotational Hamiltonian [45] and are responsible for Λ -doubling. Finally, fig. 5 reports the 10 symmetry-independent spin-orbit coupling curves obtained at the CASSCF/awc3z level. Care was taken to ensure that the coupling curves and dipoles are both smooth and phase corrected, something that is by no means standard in the literature [46].

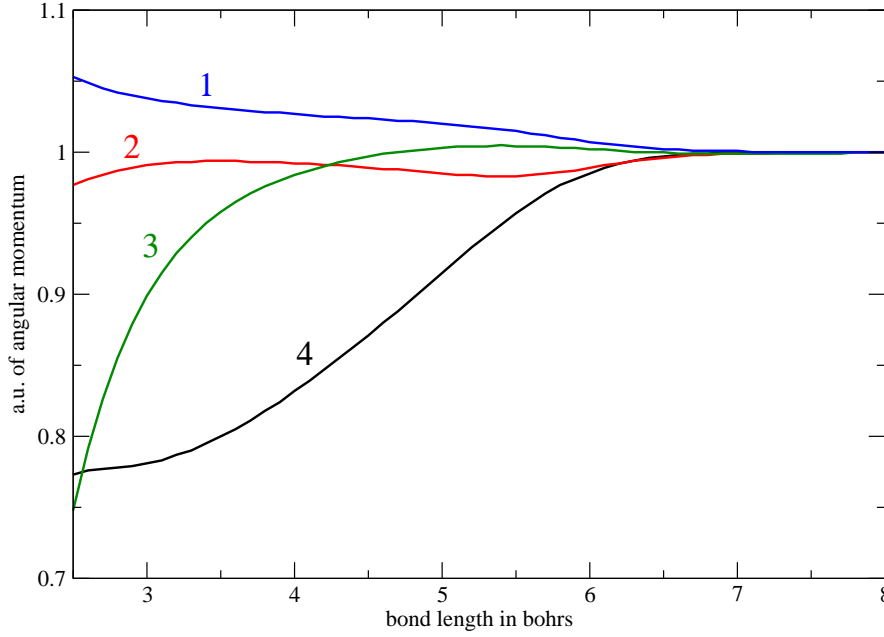


Figure 4. Matrix elements of the \hat{L}_x and \hat{L}_y operators for ScH computed with CASSCF and the awc3z basis set. Specifically, the curve labelled ‘1’ is $\langle^3\Delta_{x^2-y^2}|\hat{L}_x|^3\Pi_y\rangle/i$; curve ‘2’ is $\langle^1\Delta_{x^2-y^2}|\hat{L}_x|^1\Pi_y\rangle/(-i)$; curve ‘3’ is $\langle^3\Sigma^+|\hat{L}_y|^3\Pi_x\rangle/(\sqrt{3}i)$; curve ‘4’ is $\langle^1\Sigma^+|\hat{L}_y|^1\Pi_x\rangle/(\sqrt{3}i)$. The phases of the electronic wave functions are chosen such as $\langle^1\Pi_x|\hat{L}_z|^1\Pi_y\rangle = i$, $\langle^3\Pi_x|\hat{L}_z|^3\Pi_y\rangle = i$, $\langle^1\Delta_{x^2-y^2}|\hat{L}_z|^1\Delta_{xy}\rangle = -2i$ and $\langle^3\Delta_{x^2-y^2}|\hat{L}_z|^3\Delta_{xy}\rangle = 2i$.

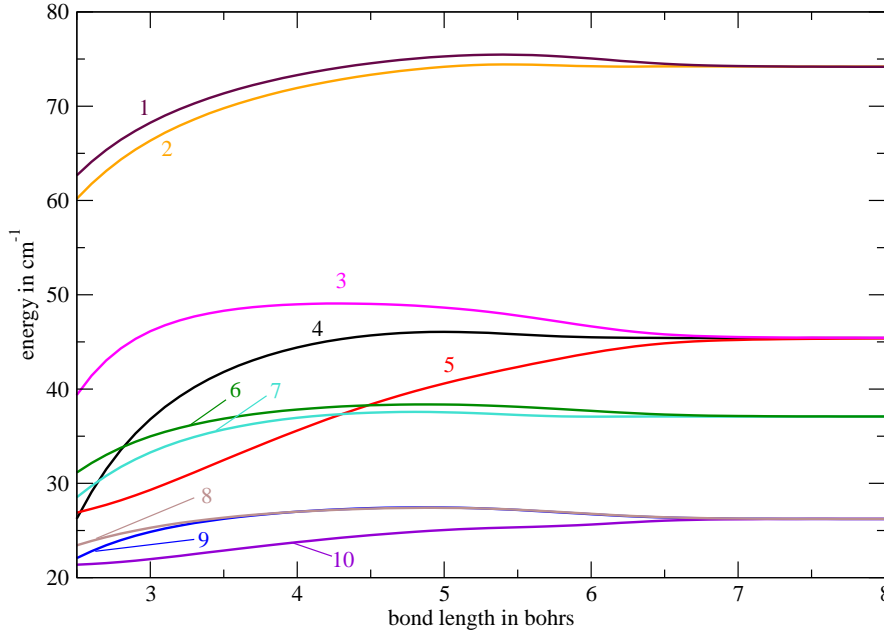


Figure 5. Spin-orbit coupling matrix elements for ScH computed with CASSCF and the awc3z basis set. Specifically: the curve labelled ‘1’ is $\langle^3\Delta_{x^2-y^2}, \Sigma = 1|\hat{H}_{SO}|^3\Delta_{xy}, \Sigma = 1\rangle/(-i)$; curve ‘2’ is $\langle^1\Delta_{xy}|\hat{H}_{SO}|^3\Delta_{xx-yy}, \Sigma = 0\rangle/(-i)$; curve ‘3’ is $\langle^3\Sigma^+, \Sigma = 0|\hat{H}_{SO}|^3\Pi_y, \Sigma = 1\rangle/(-i)$; curve ‘4’ is $\langle^1\Pi_y|\hat{H}_{SO}|^3\Sigma^+, \Sigma = 1\rangle/i$; curve ‘5’ is $\langle^1\Sigma^+|\hat{H}_{SO}|^3\Pi_y, \Sigma = 1\rangle/i$; curve ‘6’ is $\langle^3\Pi_x, \Sigma = 1|\hat{H}_{SO}|^3\Pi_y, \Sigma = 1\rangle/(-i)$; curve ‘7’ is $\langle^1\Pi_x|\hat{H}_{SO}|^3\Pi_y, \Sigma = 0\rangle/i$; curve ‘8’ is $\langle^3\Pi_x, \Sigma = 0|\hat{H}_{SO}|^3\Delta_{xy}, \Sigma = 1\rangle/i$; curve ‘9’ is $\langle^1\Delta_{xy}|\hat{H}_{SO}|^3\Pi_x, \Sigma = 1\rangle/(-i)$; curve ‘10’ is $\langle^1\Pi_y|\hat{H}_{SO}|^3\Delta_{xx-yy}, \Sigma = 1\rangle/(-i)$. The phases of the electronic wave functions are chosen such as $\langle^1\Pi_x|\hat{L}_z|^1\Pi_y\rangle = i$, $\langle^3\Pi_x|\hat{L}_z|^3\Pi_y\rangle = i$, $\langle^1\Delta_{x^2-y^2}|\hat{L}_z|^1\Delta_{xy}\rangle = -2i$ and $\langle^3\Delta_{x^2-y^2}|\hat{L}_z|^3\Delta_{xy}\rangle = 2i$.

4. Line list

The potential energy, dipole and coupling curves were then used with the in-house program DUO to produce a line list for ^{45}ScH . DUO solves in an essentially exact way the rotational-vibrational-electronic problem for multiple interacting energy curves for diatomic molecules and is described in detail elsewhere [28, 47, 48]. The line list can be obtained from www.exomol.com, while all the curves used to produce it are made available as supplementary material. In all nuclear-motion calculations we used the atomic masses $m_{\text{H}} = 1.0078250321$ Da and $m_{\text{Sc}} = 44.9559100$ Da, which give for ScH a reduced mass $\mu = (m_{\text{H}}^{-1} + m_{\text{Sc}}^{-1})^{-1} = 0.985726930$ Da = $1796.87027 m_e$.

The *ab initio* potential energy curves of the singlet terms were adjusted by fitting to the energy term values ($J \leq 12$) derived from the experimental spectroscopic constants reported by Ram and Bernath [20] which cover vibrational excitations with $v = 0, 1$ (X), $v = 0$ (A) and $v = 0, 1, 2$ (B) only. This was not possible for the triplet states (see table 4). We also decided not to use in the adjustments the very recent experimental data on the $^3\Delta$ electronic state [22] since it lead to an equilibrium bond length $r_e = 3.94 a_0$ which differs too substantially from theory to be safely trusted, see table 4.

In the refined curves the dissociation energy was fixed to the D_e value by Koseki *et al* [40]. The triplet curves were also scaled, to dissociate to the same value of D_e . All refined curves are given as supplementary material to the paper together with the *ab initio* curves. The triplet electronic states appear to be in the strong resonance with the rovibronic states from $B^1\Pi$ and prevented an accurate fit to the B -state energies, especially for $J > 12$. It should be noted however that the spectroscopic constants from Ref. [20] were derived using in the absence of the of interaction with the triplet states, and thus can also contain artifacts.

We then used the program DUO [48] to solve the coupled Schrödinger equations to compute the rovibronic energies of ScH up to the dissociation. In particular, we obtained for ^{45}ScH a zero-point-energy of 799.6 cm^{-1} . The highest value the total angular momentum J can assume for bound states is found to be $J = 59$.

The corresponding rovibronic eigenfunctions were combined with the *ab initio* dipole moment curves to produce Einstein A coefficients for all transitions with line positions up to D_0 . The Einstein A coefficients together with the rovibrational energies supplemented by the total degeneracies and quantum numbers make up the line list.

DUO calculations consist of two steps: in the first step we used a grid of 501 points to solve six separate vibrational Schrödinger equations for each electronic state, using as potential the *ab initio* potential curves shown in Fig. 1 or the empirically adjusted curves described above. We then selected 40 lowest-energy eigenfunctions from each set; the union of these $40 \times 6 = 240$ functions constitutes our vibrational basis set $|\text{state}, v\rangle$, where v is the vibrational quantum number and ‘state’ is the label identifying the electronic state. In the second step of the calculation we build

a basis set of Hund's case a functions of the type

$$|\text{state}, \Lambda, S, \Sigma, v\rangle = |\text{state}, \Lambda, S, \Sigma\rangle |J, \Omega, M\rangle |\text{state}, v\rangle, \quad (3)$$

where $|\text{state}, \Lambda, S, \Sigma\rangle$ is the electronic function, $|J, \Omega, M\rangle$ is the rotational function and $|\text{state}, v\rangle$ is one of the vibrational functions; Λ , Σ , and Ω are the z axis projections of the electronic, spin and total angular momenta, respectively, and $\Omega = \Lambda + \Sigma$; M is the projection of the total angular momentum along the laboratory axis Z . The full, coupled problem is then solved by exact diagonalization in the chosen basis set.

In order to guarantee that all phases of the *ab initio* couplings as well as transition dipole moments are consistent, we used the matrix elements of the \hat{L}_z operator between the corresponding degenerate Π and Δ components as provided by Molpro. These matrix elements were then used to transform the matrix elements of all coupling to the representation where \hat{L}_z is diagonal, which is used in DUO according with eq. (3). The phases are chosen such that all matrix elements are positive.

Our ^{45}ScH line list contains 1 152 827 transitions and is given in the ExoMol format [49] consisting of two files, an energy file and a transition file. This is based on a method originally developed for the BT2 line list [50]. Extracts for the line lists are given in Tables 8 and 9. Using all energies of ^{45}ScH we computed its partition function for temperatures up to 5000 K. The line lists and partition function together with auxiliary data including the potential energy, spin-orbit, electronic angular momentum, and dipole moment curves, as well as the absorption spectrum given in cross section format [51], can all be obtained from the ExoMol website at www.exomol.com.

As an example, in fig. 6 we show absorption ($T = 298$ K) intensities of ScH generated using a stick-diagram. Figure 7 illustrates in detail the band structure of the absorption spectrum of ScH at $T = 1\,500$ K generated using a Gaussian line profile with the half-width-at-half-maximum (HWHM) of 5 cm^{-1} . As one can see, the strongest features belong to the $X-X$, $B-X$, $a-a$, and $c-b$ electronic bands. The triplet bands electronic bands $a-a$ and $c-b$ should be strong enough to be potentially observable in the lab. Due to the spin-orbit couplings between different components forbidden bands also appear to contribute, with AX and cX being the strongest. These bands are significantly weaker than the dipole-allowed ones, but could still represent an important source of ScH opacity.

5. Conclusions

A hot line list containing pure rotational, ro-vibrational and vibronic transitions for ScH was generated using new *ab initio* potential energy, dipole moment, spin-orbit, and electronic angular moment curves obtained at a high level of theory. The work was performed with a view to astrophysical applications. The analysis of the importance of different absorption bands for the opacities of ScH is presented.

The complexity of the electronic structure problem when transition metals are

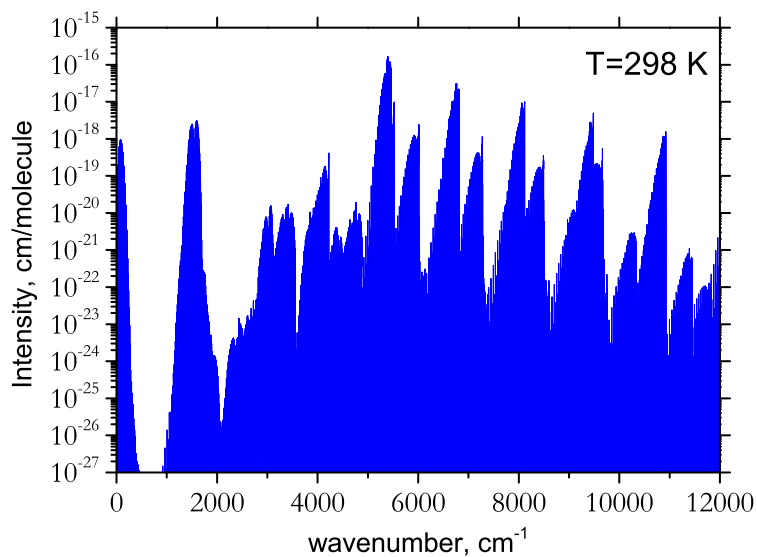
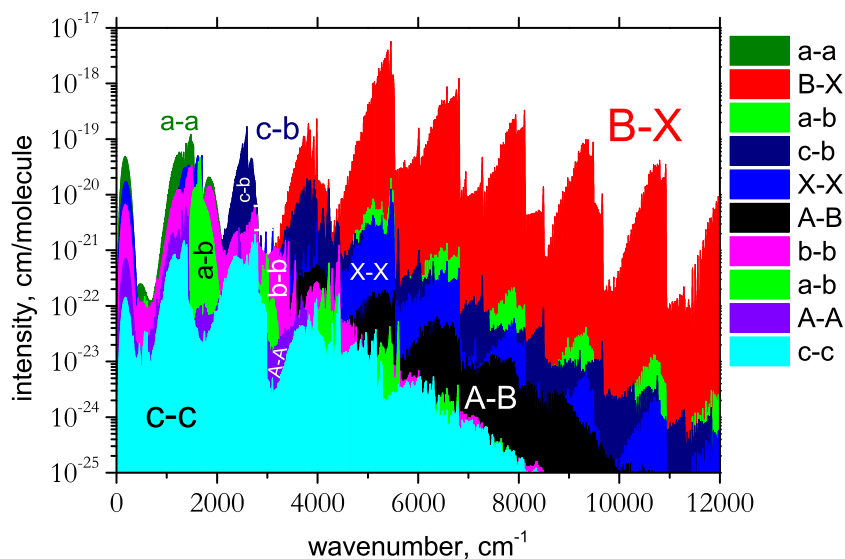
Table 8. Sample extract from the energy file for ^{45}ScH . The whole file contains 8 451 entries.

i	\tilde{E}	g	J	$+/-$	e/f	State	v	$ \Lambda $	$ \Sigma $	$ \Omega $
1	0.000000	16	0	+	f	X1Sigma+	0	0	0	0
2	1547.095548	16	0	+	f	X1Sigma+	1	0	0	0
3	3019.322250	16	0	+	f	X1Sigma+	2	0	0	0
4	3352.480112	16	0	+	f	b3Pi	0	1	1	0
5	4430.504406	16	0	+	f	X1Sigma+	3	0	0	0
6	4707.209870	16	0	+	f	b3Pi	1	1	1	0
7	5789.270187	16	0	+	f	X1Sigma+	4	0	0	0
8	6015.690883	16	0	+	f	b3Pi	2	1	1	0
9	7100.259438	16	0	+	f	X1Sigma+	5	0	0	0
10	7277.938899	16	0	+	f	b3Pi	3	1	1	0
11	8363.776161	16	0	+	f	X1Sigma+	6	0	0	0
12	8494.401968	16	0	+	f	b3Pi	4	1	1	0
13	9574.352490	16	0	+	f	X1Sigma+	7	0	0	0
14	9667.692015	16	0	+	f	b3Pi	5	1	1	0
15	10718.414759	16	0	+	f	b3Pi	6	1	1	0
16	10804.884934	16	0	+	f	X1Sigma+	8	0	0	0
17	11788.395483	16	0	+	f	b3Pi	7	1	1	0
18	11902.873682	16	0	+	f	X1Sigma+	9	0	0	0
19	12788.251034	16	0	+	f	b3Pi	8	1	1	0
20	12941.194344	16	0	+	f	X1Sigma+	10	0	0	0
21	13714.254989	16	0	+	f	b3Pi	9	1	1	0
22	13898.140315	16	0	+	f	X1Sigma+	11	0	0	0
23	14551.459500	16	0	+	f	b3Pi	10	1	1	0
24	14746.814942	16	0	+	f	X1Sigma+	12	0	0	0

 i : State counting number. \tilde{E} : State energy in cm^{-1} . g : State degeneracy. $+/-$: Actual state parity. e/f : Rotationless parity. v : State vibrational quantum number. $|\Lambda|$: Absolute value of Λ (projection of the electronic angular momentum). $|\Sigma|$: Absolute value of Σ (projection of the electronic spin). $|\Omega|$: Absolute value of $\Omega = \Lambda + \Sigma$ (projection of the total angular momentum).Table 9. Sample extract from the transition file for ^{45}ScH . The whole file contains 1 152 826 entries.

f	i	A_{if}
1351	1231	3.3006E-07
3574	3468	3.8843E-07
5782	5693	5.0269E-06
4942	5037	9.9272E-06
7688	7734	4.9607E-03
2070	1952	3.8782E-01
2919	2580	1.0196E+00
2804	2692	1.0196E+00
1362	1713	8.5042E-08
5638	5727	6.8009E-04
3137	3242	4.2340E-06
3672	3568	1.9332E-04
7406	7350	4.6729E-06
5984	5901	1.2467E-05
3396	3505	9.4844E-05
993	1110	1.0904E-06
3324	2999	1.9023E-05
2398	2282	1.0987E-04

 f : Upper (final) state counting number. i : Lower (initial) state counting number. A_{if} : Einstein A coefficient in s^{-1} .

Figure 6. Absorption cross-sections of ScH at $T=298$ K.Figure 7. Overview of the absorption line intensities of ScH at $T=1500$ K.

involved means that the accuracy of these calculations is much worse than what is normally achievable for small molecules containing light main-group elements. To help mitigate this problem, it is desirable to utilise experimental data to improve the accuracy of the results. We have done this for the singlet states.

However, for transitions involving triplet states there are no measured data for us to use: for example, the recent triplet-triplet measurements by Mukund *et al* [22] in the $17\,940\text{ cm}^{-1}$ region lie well above our calculated transitions and have not reported any absolute energies of the lower $a^3\Delta$ electronic state. Besides, their

only parameter with which we can directly compare, B_e , appears to be too low to be fully trusted. Thus for the triplet states we used the T_e valued taken from our *ab initio* calculations, which may be in error by up to a few thousands cm^{-1} , implying that the entire bands may be erroneously shifted by similar amounts. Also, structure due to perturbations in both the singlet and triplet manifolds are dependent on the potential energy curve separations and therefore may not be reproduced accurately. However we expect that our line list to be quantitatively accurate enough for the singlet state energies and to provide a detailed spectral structure of individual bands to be useful.

Acknowledgements

This work was supported by ERC Advanced Investigator Project 267219.

References

- [1] R.E. Smith, Proc. R. Soc. Lon. Ser.A **332**, 113 (1973).
- [2] P.R. Scott and W.G. Richards, J. Phys. B: At. Mol. Opt. Phys. **7**, 1679 (1974).
- [3] P.R. Scott and W.G. Richards, The electronic structure of diatomic transition-metal molecules. in *Molecular Spectroscopy: Volume 4*, edited by R F Barrow, D A Long and J Sheridan, Vol. 4 (The Royal Society of Chemistry, Cambridge, UK, 1976), pp. 70–95.
- [4] A.B. Kunz, M.P. Guse and R.J. Blint, J. Phys.B: At. Mol. Phys. **8**, L358 (1975).
- [5] G. Das, J. Chem. Phys. **74**, 5766 (1981).
- [6] J.T. Hougen, J. Mol. Spectrosc. **267**, 23 (2011).
- [7] P. Pyrkko, Phys. Scr. **20**, 647 (1979).
- [8] C.W. Bauschlicher and S.P. Walch, J. Chem. Phys. **76**, 4560 (1982).
- [9] G.H. Jeung and J. Koutecky, J. Chem. Phys. **88**, 3747 (1988).
- [10] J. Anglada, P.J. Bruna, S.D. Peyerimhoff and R.J. Buenker, J. Molec. Struct. (THEOCHEM) **10**, 299 (1983).
- [11] J. Anglada, P.J. Bruna, S.D. Peyerimhoff and R.J. Buenker, J. Molec. Struct. (THEOCHEM) **107**, 163 (1984).
- [12] P.J. Bruna and J. Anglada, Low-Lying Electronic States of Sch, TiH and VH according to MRD-CI calculations. in *Quantum Chemistry: The Challenge of Transition Metals and Coordination Chemistry*, edited by A Veillard, *NATO ASI Series*, Vol. 176 (Springer, Dordrecht, The Netherlands, 1986), pp. 67–78.
- [13] J. Anglada, P.J. Bruna and S.D. Peyerimhoff, Mol. Phys. **66**, 541 (1989).
- [14] J.Z. Guo and J.M. Goodings, J. Molec. Struct. (THEOCHEM) **549**, 261 (2001).
- [15] S. Goel and A.E. Masunov, J. Chem. Phys. **214302**, 129 (2008).
- [16] M. Hubert, J. Olsen, J. Loras and T. Fleig, J. Chem. Phys. **139**, 194106 (2013).
- [17] D.P. Chong, S.R. Langhoff, C.W. Bauschlicher, S.P. Walch and H. Partridge, J. Chem. Phys. **85**, 2850 (1986).
- [18] A. Bernard, C. Effantin and R. Bacis, Can. J. Phys. **55**, 1654 (1977).
- [19] R.S. Ram and P.F. Bernath, J. Chem. Phys. **105**, 2668 (1996).
- [20] R.S. Ram and P.F. Bernath, J. Mol. Spectrosc. **183**, 263 (1997).
- [21] A. Le and T.C. Steimle, J. Phys. Chem. A **115**, 9370 (2011).
- [22] S. Mukund, S. Bhattacharyya and S.G. Nakhate, J. Quant. Spectrosc. Radiat. Transf. **147**, 274 (2014).
- [23] J. Tennyson and S.N. Yurchenko, Mon. Not. R. Astron. Soc. **425**, 21 (2012).
- [24] B. Yadin, T. Vaness, P. Conti, C. Hill, S.N. Yurchenko and J. Tennyson, Mon. Not. R. Astron. Soc. **425**, 34 (2012).
- [25] E.J. Barton, S.N. Yurchenko and J. Tennyson, Mon. Not. R. Astron. Soc. **434**, 1469 (2013).
- [26] E.J. Barton, C. Chiu, S. Golpayegani, S.N. Yurchenko, J. Tennyson, D.J. Frohman and P.F. Bernath, Mon. Not. R. Astron. Soc. **442**, 1821 (2014).
- [27] L. Yorke, S.N. Yurchenko, L. Lodi and J. Tennyson, Mon. Not. R. Astron. Soc. **445**, 1383 (2014).
- [28] A.T. Patrascu, J. Tennyson and S.N. Yurchenko, Mon. Not. R. Astron. Soc. (2015).

- [29] F. Allard, P.H. Hauschildt, D.R. Alexander and S. Starrfield, *Annu. Rev. Astron. Astrophys.* **35**, 137 (1997).
- [30] K. Lodders, *Astrophys. J.* **591**, 1220 (2003).
- [31] H.J. Werner, P.J. Knowles, G. Knizia, F.R. Manby and M. Schütz, *WIREs Comput. Mol. Sci.* **2**, 242 (2012).
- [32] A. Kramida, Y. Ralchenko and J. Reader, NIST Atomic Spectra Database – Version 5 2013, <http://www.nist.gov/pml/data/asd.cfm>.
- [33] N.B. Balabanov and K.A. Peterson, *J. Chem. Phys.* **123**, 064107 (2005).
- [34] N.B. Balabanov and K.A. Peterson, *J. Chem. Phys.* **125**, 074110 (2006).
- [35] J. Raab and B.O. Roos, *Adv. Quant. Chem* **48**, 421 (2005).
- [36] N.J. Mayhall, K. Raghavachari, P.C. Redfern, L.A. Curtiss and V. Rassolov, *J. Chem. Phys.* **128**, 144122 (2008).
- [37] H.J. Werner and P.J. Knowles, *Journal of Chemical Physics* **89**, 5803 (1988).
- [38] C.M. Western, PGOPHER 8.0, A program for simulating rotational structure 2013, University of Bristol, <http://pgopher.chm.bris.ac.uk>.
- [39] MRCC, a string-based quantum chemical program suite written by M. Kállay. See also M. Kállay and P. R. Surján, *J. Chem. Phys.*, **115**, 2945 (2001), as well as: www.mrcc.hu.
- [40] A. Kant and K.A. Moon, *High Temp. Sci.* **14**, 23 (1981).
- [41] S. Koseki, Y. Ishihara, D.G. Fedorov, H. Umeda, M.W. Schmidt and M.S. Gordon, *J. Phys. Chem. A* **108**, 4707 (2004).
- [42] A.E. Lynas-Gray, S. Miller and J. Tennyson, *J. Mol. Spectrosc.* **169**, 458 (1995).
- [43] L. Lodi and J. Tennyson, *J. Phys. B: At. Mol. Opt. Phys.* **43**, 133001 (2010).
- [44] S.O. Adamson, A. Zaitsevskii and N.F. Stepanov, *J. Phys. B: At. Mol. Opt. Phys.* **31**, 5275 (1998).
- [45] H. Lefebvre-Brion and R.W. Field, *Perturbations in the spectra of diatomic molecules* (Academic Press, Orlando FL, USA, 1986).
- [46] J. Tennyson, *J. Mol. Spectrosc.* **298**, 1 (2014).
- [47] A.T. Patrascu, C. Hill, J. Tennyson and S.N. Yurchenko, *J. Chem. Phys.* **141**, 144312 (2014).
- [48] S.N. Yurchenko, L. Lodi, J. Tennyson and A.V. Stolyarov, *Comput. Phys. Commun.* (2015).
- [49] J. Tennyson, C. Hill and S.N. Yurchenko, Data structures for ExoMol: Molecular line lists for exoplanet and other atmospheres. in *6th international conference on atomic and molecular data and their applications ICAMDATA-2012, AIP Conference Proceedings*, Vol. 1545 (2013), pp. 186–195.
- [50] R.J. Barber, J. Tennyson, G.J. Harris and R.N. Tolchenov, *Mon. Not. R. Astron. Soc.* **368**, 1087 (2006).
- [51] C. Hill, S.N. Yurchenko and J. Tennyson, *Icarus* **226**, 1673 (2013).